

# A General Framework for RIS-Aided mmWave Communication Networks: Channel Estimation and Mobile User Tracking

Salah Eddine Zegrar, Liza Afeef, and Hüseyin Arslan, *Fellow, IEEE*

**Abstract**—Reconfigurable intelligent surface (RIS) has been widely discussed as new technology to improve wireless communication performance. Based on the unique design of RIS, its elements can reflect, refract, absorb, or focus the incoming waves toward any desired direction. These functionalities turned out to be a major solution to overcome millimeter-wave (mmWave)s high propagation conditions including path attenuation and blockage. However, channel estimation in RIS-aided communication is still a major concern due to the passive nature of RIS elements, and estimation overhead that arises with multiple-input multiple-output (MIMO) system. As a consequence, user tracking has not been analyzed yet. This paper is the first work that addresses channel estimation, beamforming, and user tracking under practical mmWave RIS-MIMO systems. By providing the mathematical relation of RIS design with a MIMO system, a three-stage framework is presented. Starting with estimating the channel between a base station (BS) and RIS using hierarchical beam searching, followed by estimating the channel between RIS and user using an iterative resolution algorithm. Lastly, a popular tracking algorithm is employed to track channel parameters between the RIS and the user. System analysis demonstrates the robustness and the effectiveness of the proposed framework in real-time scenarios.

**Index Terms**—Reconfigurable intelligent surfaces, mmWave, channel estimation, beamforming, user tracking.

## I. INTRODUCTION

MILLIMETER-WAVE (mmWave) communication has become one of the key technologies of fifth-generation (5G) communication systems. Although mmWave achieves high data rate due to its wider signal bandwidth, it suffers from severe path loss [1]. Many solutions can be implemented to overcome these losses including high-dimensional multiple-input multiple-output (MIMO) operations, and reconfigurable intelligent surface (RIS) technology to mitigate the limitation conditions of high frequencies. Recently, RIS has attracted much attention as a highly promising technology that can meet the requirements of the sixth-generation (6G) and beyond wireless networks. RISs capability arises from its ability to support MIMO systems in controlling and hardening the wireless channel, where a highly time-varying channel can

behave as a deterministic one. The functionalities of RIS including reflecting, diffracting, or scattering the transmitted signal enhance the quality of the signal at the receiver side. These abilities come from its unique design where the adjustable passive elements can individually steer the incident electromagnetic (EM) wave toward any specific direction by changing their phases and gains only. Adjusting these elements allows us to align all multipath of the reflected signal so that they are added constructively at the receiver [2]. This principle of the RIS elements fulfills the concepts of beamforming and steering concepts [3], [4]. Therefore, with proper RIS size and reflection coefficients, the reflected signal is a beam, where the width of this beam is inversely proportional to the size of the RIS. Since these elements passively reflect the signal, they are easy to implement, have a low-cost deployment, and most importantly do not cause noise amplification [5]. These features makes the RIS a strong candidate in upcoming wireless systems over conventional technologies.

On the other side, RIS imposes a lot of challenges such as channel estimation. Since the RIS is built of a large number of passive elements, RIS-aided communication networks have faced difficulties in estimating the channel reliably. To overcome these difficulties, many channel estimation techniques have been proposed in the literature under different approaches.

In single-user systems, [6] proposes a novel RIS architecture in which some of its elements are active by connecting them to a baseband processor. These active elements turned back to the reflecting mode after estimating the channel. However, this sensor deployment, that activates the elements, increases the implementation cost. Prior works [7]–[14] focused on introducing channel estimation techniques with fully passive RIS elements. A two-stage algorithm, in [7], for channel estimation is proposed. In the first stage, all RIS elements are turned off whereas the direct channel between the base station (BS) and user equipment (UE) is estimated. Then, in the second stage, the elements are turned on one by one while the channel between each element and UE is being estimated. In spite of that, this strategy degrades the channel estimation accuracy since only a small portion of RIS elements are switched on at each time. This also requires using a separate amplitude control and phase shifter for each element which increases the system cost, especially for a massive number of RIS elements. Therefore, the approach in [8] divides the RIS elements  $N$  into  $M$  sub-surfaces while keeping the elements on with maximum reflected amplitude during the channel estimation and data

The authors are with the Department of Electrical and Electronics Engineering, Istanbul Medipol University, Istanbul, 34810, Turkey (e-mail: salah.zegrar@std.medipol.edu.tr; liza.shehab@std.medipol.edu.tr; huseyinarslan@medipol.edu.tr).

H. Arslan is also with Department of Electrical Engineering, University of South Florida, Tampa, FL, 33620, USA.

This work has been submitted to the IEEE for possible publication. Copyright may be transferred without notice, after which this version may no longer be accessible.

transmission. Each sub-surface consists of  $N/M$  adjacent elements with a common reflection coefficient to reduce the implementation complexity. Following the same approach, [9] proposes a discrete Fourier transform (DFT)-based channel estimation method where all the RIS elements are on at all time slots and the DFT matrix is used to determine the reflection coefficients of these elements. In addition, minimum mean squared error (MMSE) algorithm is proposed in [10] to work with DFT matrix to estimate the channel of both direct path and the RIS-assisted path between the BS and UE in multiple-input single-output (MISO) system. For more realistic setting, [11] considers discrete-phase RIS reflecting elements that are grouped into a relatively small number of sub-surfaces, and proposes a DFT-Hadamard-based reflection pattern strategy to minimize the channel estimation error in imperfect channel state information (CSI). However, increasing the number of sub-surfaces causes training overhead and degradation in the spectrum efficiency. Meanwhile, free-space path loss models for the RIS-assisted wireless communication are proposed in [3], [15] using the EM and physical properties of a reconfigurable surface. In [3], a two-dimensional (2D) path loss model is derived and extended to three-dimensional (3D) one in [15] including far-field, near-field beamforming, and near-field broadcasting formulas are experimentally validated in the indoor environment.

In a multiuser system, [12] investigates the MISO system under imperfect CSI, where it considers correlated Rayleigh fading channel. The proposed protocol utilizes DFT-MMSE estimation and divides channel estimation into subphases, at each one, all users transmit orthogonal pilot symbols to estimate the RIS-assisted links. The work in [13] proposes a three-phase channel estimation framework for the RIS-assisted uplink MISO system to reduce the training duration. In phase one, RIS elements are turned off and direct channels between UEs and BS are estimated. Then, in the next phase, among all UEs, only one UE transmitted pilots and the cascaded channel is estimated. In the last phase, the channel between all UEs and the RIS is considered correlated, thus only the scaling factors need to be estimated. However, the training overhead, the number of supportable users, and the performance of channel estimation are the limits of this technique.

In mmWave systems, channel estimation becomes more critical with few works touching this problem [6], [14], [16], [17]. The work in [14] proposes a compressed-sensing-based channel estimation algorithm where the sparsity of the channel is exploited to implement channel estimation at a reduced pilot overhead in massive MIMO system. The sparsity of the channel is capitalized using a distributed orthogonal matching pursuit algorithm. It is assumed that there is prior knowledge about the channel between the BS and the RIS, and the pilots are designed accordingly. However, considering the channel BS-RIS to be known and time-invariant are not practical since mmWave channel is sensitive to small changes. Similarly, a compressed sensing algorithm is utilized in [18] to estimate the cascaded channel parameters in the RIS-assisted THz MIMO system in the indoor application scenarios, since it is assumed that the estimation problem is equivalent to sparse recovery problem. Again, using the same method, [19] tries to find

a sparse representation of the cascaded BS-RIS-UE channel in mmWave downlink system with the help of transposed Khari-Rao product and Kronecker product. The most recent work for channel estimation in mmWave systems was in [20], where a two-stage cascaded channel estimation protocol is proposed by exploiting the sparsity of mmWave MIMO channel of single BS, RIS, and UE. In the first stage, the beam searching approach is introduced to have high angular domain information, then in a second stage, an adaptive grid matching pursuit algorithm is proposed to estimate the high-resolution cascaded channel. However, estimating a cascaded channel has many limitations as it will be explained and proved later in this paper.

Although the aforementioned channel estimation techniques are theoretically effective with low mean square error (MSE) level, they depend on either cascaded channel concept or non-practical assumptions for estimating the channel BS-RIS-UE. Since RIS reflects the signal and focuses the energy into a specific direction, UE's location should be considered in the estimation process. However, in [6]–[14], [16]–[19], the location is always ignored and only scenarios with stationary BS, RIS and UE are considered. Furthermore, it is proven in [3], [15] that the path loss is a function of reflection coefficients of RIS which is always ignored in the channel estimation process when the phases are optimized for channel estimation.

In this article, we develop a general three-stage framework for the RIS-aided communication network, where practical issues are considered in a realistic scenario. We summarize the main contributions of this paper as follows

- First, we derive the relation between RIS and MIMO system by providing an accurate configuration for the RIS reflection coefficients array, noting that the resultant array is equivalent to the steering vector of the MIMO system that has uniform planner array (UPA) in its antenna structure. The derived model for the RIS is obtained from the free space far-field path loss model that is introduced in [15].
- Additionally, we optimize the reflected signal in any specific direction simply by controlling the phases, where the effect of channel BS-RIS is eliminated at the BS side, and the UE has the responsibility of estimating and compensating channel RIS-UE. For the first time, this optimization proposes one channel control (BS-RIS) for the RIS design instead of endeavoring the total cascaded channel control.
- Next, a novel channel estimation scheme for mmWave RIS-MIMO system is proposed. This scheme is able to estimate both BS-RIS and RIS-UE channels separately, even though all RIS elements are passive. Starting with estimating the BS-RIS channel  $\mathbf{G}$  using hierarchical beam searching algorithm. Then, the RIS-UE channel  $\mathbf{H}$  is estimated by adopting the iterative reweight algorithm that is introduced in [21] to estimate the channel path coefficients only, exploiting the resultant angles from the beam searching algorithm.
- Then, the proposed scheme enables RIS-assisted communication to track mobile users. To the best of our

knowledge, this has never been addressed in the literature and it is considered one of the most challenging tasks to be implemented by the RIS. The parameters of channel  $\mathbf{H}$  are tracked using well-known algorithms such as the extended Kalman filter (EKF) algorithm.

- Finally, the mmWave RIS-MIMO framework is studied under practical and implementable assumptions. The proposed design of the RIS reflection coefficients has low computational complexity and applicable in real-time scenarios. Meanwhile, all channel effects are considered in the design including path loss, fading, user's location, incident and reflected angles. We analytically show that our proposed design achieves better performance compared to the conventional methods under the same assumptions.

The rest of this paper is organized as follows. Section II discusses some assumptions available in the literature. Section III depicts the system model of the proposed RIS framework, and Section IV discusses how to control the RIS's reflection coefficients to realize beamforming/steering functionalities. The novel channel estimation scheme is introduced in Section V followed by channel tracking approaches. In Section VI, the performance analysis is carried out, and Section VII concludes the paper.

*Notation:* bold uppercase  $\mathbf{A}$ , bold lowercase  $\mathbf{a}$ , and unbold letters  $A, a$  are used to denote matrices, column vectors, and scale values, respectively.  $|a|$  and  $\angle a$  are the magnitude and phase of a complex number.  $\|\mathbf{a}\|_F$ ,  $\|\mathbf{a}\|_0$ , and  $\|\mathbf{a}\|_2$  are the Frobenius norm,  $\ell_0$  pseudo-norm, and the  $\ell_2$  norm.  $(\cdot)^H$ ,  $(\cdot)^T$ , and  $(\cdot)^{-1}$  denote the Hermitian transpose, transpose, and inverse.  $\text{diag}(\mathbf{a})$  is the diagonal matrix with the vector  $\mathbf{a}$  on its diagonal.  $\mathbb{C}^{M \times N}$  denotes the space of  $M \times N$  complex-valued matrices and  $\text{vec}(\mathbf{A})$  is vectorizing the matrix  $\mathbf{A}$ .  $A \otimes B$  is the Kronecker product of  $A$  and  $B$  and symbol  $j$  represents the imaginary unit of complex numbers with  $j^2 = -1$ .

## II. INVESTIGATION ABOUT RIS

In this section, three major concerns are discussed regarding path loss, channel model, and user tracking in RIS-assisted networks.

*A. If multipath, path loss, and beamforming are to be optimized at the same time, what should be the reflection coefficients of the RIS?*

Prior works have investigated RIS phases matrix based on different criteria. Some authors [3], [15], [22] specified the RIS matrix  $\phi$  so that the path loss is minimized, while others [5], [8], [11], [13] used these phases to align all multipath and get rid of channel effects. And some other authors designed  $\phi$  for decreasing the error in channel estimation. Eventually, using the same parameters for multiple purposes at the same time will create a conflict, and in this case, one general multi-goal design of the phases is required.

Assuming that the RIS elements are placed in a uniform rectangular shape, then the reflection coefficients of these

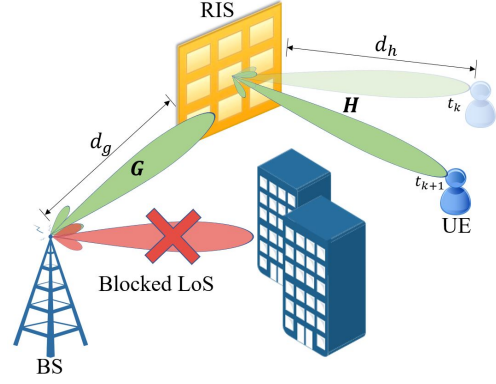


Fig. 1: RIS-aided communication system model.

elements is reflected by

$$\phi = \begin{bmatrix} \phi_{1,1} & \phi_{1,2} & \cdots & \phi_{1,N_{RIS}} \\ \vdots & \ddots & & \vdots \\ \phi_{N_{RIS},1} & \phi_{N_{RIS},2} & \cdots & \phi_{N_{RIS},N_{RIS}} \end{bmatrix}, \quad (1)$$

where  $\phi_{n,m} = \gamma_{n,m} e^{j\alpha_{n,m}}$  is the  $(n,m)$ -th RIS element's reflection coefficient, where  $\alpha_{n,m} \in [0, 2\pi)$  represents the phase shift induced by the  $(n,m)$ -th element in the RIS, and  $\gamma_{n,m} \in [0, 1]$  stands for the reflection gain which will be considered unity throughout the paper i.e.,  $\gamma_{n,m} = 1, \forall (n,m)$ . Another convenient representation of  $\phi$  in term of facilitating computations is defined as  $\Theta = \text{diag}\{\text{vec}(\phi)\}$ .

Considering the system model that is shown in Fig. 1, the reflected signals from each element of the RIS are all aligned in phase to enhance the received signal power. It is assumed that the direction of the radiation is toward the center of the RIS surface. For more simplification, let the dimensions of the each element be  $d_x \times d_x$  and the total number is  $M_{RIS} = N_{RIS} \times N_{RIS}$  elements. In this case, the free-space path loss is given as [15]

$$\beta_{RIS} = \frac{G_t G_r G_{N_{RIS}}^4 d_x^2 \lambda^2 F(\theta_t, \varphi_t) F(\theta_r, \varphi_r) \gamma^2}{64\pi^3 d_g^2 d_h^2} \times \left| \frac{\text{sinc}\left(\frac{\pi N_{RIS}}{\lambda} (\sin \theta_t \cos \varphi_t + \sin \theta_r \cos \varphi_r + \delta_1) d_x\right)}{\text{sinc}\left(\frac{\pi}{\lambda} (\sin \theta_t \cos \varphi_t + \sin \theta_r \cos \varphi_r + \delta_1) d_x\right)} \right| \frac{\text{sinc}\left(\frac{\pi N_{RIS}}{\lambda} (\sin \theta_t \sin \varphi_t + \sin \theta_r \sin \varphi_r + \delta_2) d_x\right)}{\text{sinc}\left(\frac{\pi}{\lambda} (\sin \theta_t \sin \varphi_t + \sin \theta_r \sin \varphi_r + \delta_2) d_x\right)}, \quad (2)$$

where  $\delta_1 (m - \frac{1}{2}) d_x + \delta_2 (n - \frac{1}{2}) d_y = \frac{\lambda \phi_{n,m}}{2\pi}$ ,  $G_t, G_r$  and  $G$  are the gains of the transmitter antenna, receiver antenna, and the RIS, respectively,  $\lambda$  is the wavelength,  $F(\theta, \varphi)$  is the normalized power radiation,  $(\theta_t, \varphi_t)$  and  $(\theta_r, \varphi_r)$  represent the elevation and the azimuth angles of the incidence wave and reflected wave, respectively, and  $d_g$  and  $d_h$  are the distance from the BS to the RIS and from the RIS to the UE respectively. Let  $(\theta_{des}, \varphi_{des})$  be the angle from the RIS to UE, if  $\theta_r = \theta_{des}$  and  $\varphi_r = \varphi_{des}$ , then (2) is maximized as

$$\beta_{max}(d, \theta, \varphi) = \frac{G_t G_r G_{N_{RIS}}^4 d_x^2 \lambda^2 F(\theta_t, \varphi_t) F(\theta_r, \varphi_r) \gamma^2}{64\pi^3 d_g^2 d_h^2}. \quad (3)$$

TABLE I: Impact of  $\phi$  design on the received power

Case	Received signal's power $P_r$
Ideal/desired case	$P_r \propto \frac{M_{RIS}^2}{d_g^2 d_h^2}$
$\phi = \phi^1$	$P_r \propto \frac{A}{d_g^2 d_h^2}, A \in [0, M_{RIS}^2]$
$\phi = \phi^2$	$P_r \propto B \frac{M_{RIS}^2}{d_g^2 d_h^2}, B \in [0, 1]$
$\phi = \phi^3$	$P_r \propto \frac{AB}{d_g^2 d_h^2}$
Infinite reflector	$P_r \propto \frac{B}{(d_g + d_h)^2}$ [23]

This corresponds to the phases of the RIS  $\phi_{n,m}$  being designed as follows

$$\angle \phi_{n,m}^1 = \text{mod} \left( -\frac{2\pi}{\lambda} d_x \left[ (\sin \theta_t \cos \varphi_t + \sin \theta_{des} \cos \varphi_{des}) \left( m - \frac{1}{2} \right) + (\sin \theta_t \sin \varphi_t + \sin \theta_{des} \sin \varphi_{des}) \left( n - \frac{1}{2} \right) \right], 2\pi \right). \quad (4)$$

Fig. 2a shows the radiation pattern of the reflected signal when  $\phi$  is set to reflect the received signal in a specific direction  $(\theta_{des}, \varphi_{des}) = (45^\circ, 60^\circ)$ , the power is focused in the desired direction and diminishes elsewhere.

RIS phases are optimized to obtain strongest channel impulse response

$$\phi_{n,m}^2 = \max_{\phi} \left( \left| \sum_{n=1}^N \sum_{m=1}^M \phi_{n,m} G_{n,m} H_{n,m} \right|^2 \right), \quad (5)$$

which implies  $\phi_{n,m}^2 = -\angle \mathbf{G}_{n,m} \mathbf{H}_{n,m}$ . In the same paper [8] however, in channel estimation,  $\phi$  is chosen so that channel estimation error is minimized, for instance, the authors in [12] claim that for minimizing MSE, the reflection pattern of the RIS should be chosen to be  $N_{RIS} \times N_{RIS}$  DFT matrix  $\phi_{n,m}^3 = DFT^{N_{RIS} \times N_{RIS}}$ . It is clearly seen that there is a contradiction of  $\phi^1 \neq \phi^2 \neq \phi^3$ .

*“In case of  $\phi = DFT^{N_{RIS} \times N_{RIS}}$ , is it guaranteed that all multipath are aligned, and the signal is reflected toward the direction of user with maximum power, i.e.,  $P_r \propto M_{RIS}^2 \times \beta_{max}$ ? If not, up to what extent the estimated channel is reliable? And if some power is received, what ensures that the source of this power is the RIS and not other random reflectors?”*

Table I summarizes all the above-mentioned cases of different RISs' phases matrices compared to the ideal desired case. From this Table, it is concluded that for reliable channel estimation and communication using RIS, the RIS's phases must be optimized taking into consideration beamforming/steering direction (UE's location) and the impact of channels  $\mathbf{H}$  and  $\mathbf{G}$ . All the mentioned points here will be examined in detail in Section V.

**B. What is the impact of channel  $\mathbf{H}$  and  $\mathbf{G}$  on the RIS phases? Is it the same or different?**

Using what was discussed in Section II-A, and the basic properties of RIS that are mentioned and proved in [3], [4], let it is assumed a scenario where a signal is going to be reflected toward the same location as shown in Fig. 2a with

the assumption that  $\mathbf{G}$  is an ideal channel i.e., it has unitary gain. The predefined values of the phases would be given by (3), and the resulted radiation will be exactly as in Fig. 2a. However, when  $\mathbf{G}$  is assumed to be a sparse channel where line-of-sight (LoS) path between BS and RIS is the dominant path, it is observed that the beam is shifted toward a different direction than that of UE's location as shown in Fig. 2b. Also, when channel  $\mathbf{G}$  is very rich scattering, the UE will receive very low power from RIS as shown in Fig. 2c, and in this case, the RIS may react worse than a normal reflector (metallic surface, wall, etc.) [6]. Therefore, for a **successful reflection**,  $\mathbf{G}$  should be individually estimated and then equalized at the RIS by simply reversing its effect.

After reflecting the beam, the UE estimates and equalizes  $\mathbf{H}$  to complete a **successful communication**. In a nutshell, RIS performs two operations separately

- 1) **Accumulation**, where it collects all the energy received by each of its elements<sup>1</sup> and then align them by cancelling the effects of channel  $\mathbf{G}$ .
- 2) **Beamforming/Steering**, the RIS acts like a virtual BS, and focuses or steers the incoming electromagnetic waves using (4) toward the UE's location [22].

*C. Assuming that our system has mobility, which part of the cascaded channel is considered varying;  $\mathbf{G}$ ,  $\mathbf{H}$ , or both? Can the UE be tracked if the varying source is unknown?*

The majority of the state-of-art considers the user to be stationary, and BS have always LoS with RIS. However, these assumptions are not realistic, and tend to limit the use of RIS. Besides, they are the consequence of utilizing the cascaded channel model that is given by  $\mathbf{H}_{cascaded} \triangleq \mathbf{G}\mathbf{H}$ . This representation makes channel tracking in time almost impossible, since any change in  $\mathbf{H}_{cascaded}$  could be due to the change in  $\mathbf{G}$ ,  $\mathbf{H}$  or both. Also, in Section II-B, it was shown that only  $\mathbf{G}$  affects the phases of the RIS, not  $\mathbf{H}$ . Furthermore, if  $\mathbf{G}$  is estimated separately, estimating  $\mathbf{H}$  is feasible and tracking UEs becomes possible. Consequently, the assumption of having a mobile user is valid. For instance, the authors in [14] claim that it is almost impossible to estimate  $\mathbf{G}$  via conventional channel estimation schemes, since the RIS elements are passive. This claim will be disproved during this work.

### III. SYSTEM MODEL

Consider a narrowband mmWave MIMO system, composed of one BS, one RIS and  $k$  UEs as depicted in Fig.1. Each, BS, RIS and UE, are equipped with equidistant UPAs as an antenna structure with half-wavelengthed distance between the antenna elements in which they have  $M_{BS}$ ,  $M_{RIS}$ , and  $M_{UE}$  antenna elements, respectively. It is considered that the uplink and downlink transmissions are using a time-division duplexing (TDD) protocol that exploiting channel reciprocity for the CSI acquisition at the RIS in both link directions. The BS is assumed to have  $M_{RF}$  radio-frequency (RF) chains where the number of these chains is much smaller than the

<sup>1</sup>This is the reason why the gain is proportional to  $M_{RIS}^2$  [3]

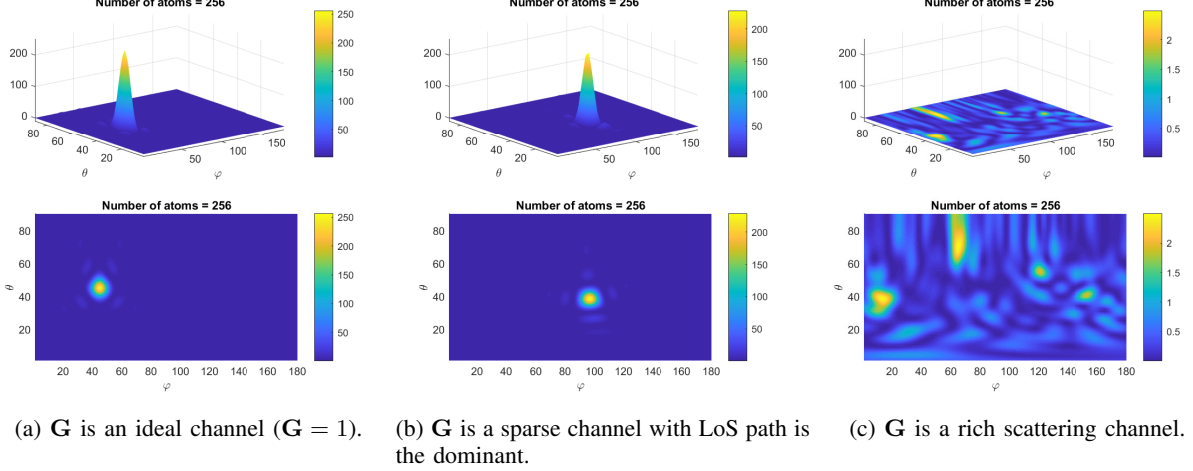


Fig. 2: The power pattern of the reflected beam from the RIS toward UE under three conditions of channel  $\mathbf{G}$

antenna array elements and larger than the number of UEs ( $k \leq M_{\text{RF}} \ll M_{\text{BS}}$ ) [24], while the UE consists of only one RF chain. The RIS is placed near to the UE side and far from the BS to minimize the path loss effect [15]. In order to fully utilize the functionality of the RIS, the channel path between the BS and UE is assumed to be blocked by an obstacle. The RIS structure is the same as the one proposed in Section II-A.

Assuming that  $s$  training symbols are transmitted via orthogonal precoding beams for each user, such that there is no inter-user interference. Under this assumption, we shall restrict the analysis to one representative UE without loss of generality. Under the assumption of flat-fading and perfect timing and frequency synchronization [25], the sparsity of the channel is exploited by using geometric channel modeling [26], [27], giving that  $\mathbf{G} \in \mathbb{C}^{M_{\text{RIS}} \times M_{\text{BS}}}$  and  $\mathbf{H} \in \mathbb{C}^{M_{\text{UE}} \times M_{\text{RIS}}}$  denote the channel between BS-RIS and RIS-UE, respectively. The  $\mathbf{G}$  model is given as

$$\mathbf{G} = \sum_{l=1}^{L_g} z_{g,l} \mathbf{a}_{\text{M}_{\text{RIS}}}(\theta_{g,l}^R, \varphi_{g,l}^R) \mathbf{a}_{\text{M}_{\text{BS}}}^H(\theta_{g,l}^B, \varphi_{g,l}^B), \quad (6)$$

$$= \mathbf{A}_{\text{M}_{\text{RIS}}}(\Omega_R) \text{diag}(\mathbf{z}_g) \mathbf{A}_{\text{M}_{\text{BS}}}^H(\Omega_B),$$

where  $L_g$  is the number of channel paths received at the RIS,  $\theta_{g,l}^R, \varphi_{g,l}^R$  and  $\theta_{g,l}^B, \varphi_{g,l}^B$  are the elevation and azimuth angles of angle of arrival (AoA) and angle of departure (AoD) in each path, and  $z_{g,l}$  is the complex channel coefficient between BS-RIS at  $l$ th path.  $\mathbf{z}_g = [z_{g,1}, z_{g,2}, \dots, z_{g,L_g}]^T$ ,  $\Omega_R = [(\theta_{g,1}^R, \varphi_{g,1}^R), (\theta_{g,2}^R, \varphi_{g,2}^R), \dots, (\theta_{g,L_g}^R, \varphi_{g,L_g}^R)]^T$ , and  $\Omega_B = [(\theta_{g,1}^B, \varphi_{g,1}^B), (\theta_{g,2}^B, \varphi_{g,2}^B), \dots, (\theta_{g,L_g}^B, \varphi_{g,L_g}^B)]$ .  $\mathbf{a}_{\text{M}_{\text{RIS}}}$  is the array response vector of the UPA [28] represented by

$$\mathbf{a}_{M_i}(\theta, \varphi) = \frac{1}{\sqrt{M_i}} \left( \mathbf{q}(\sin(\theta) \cos(\varphi)) \otimes \mathbf{p}(\sin(\theta) \sin(\varphi)) \right), \quad (7)$$

where  $\mathbf{q}(u) = [1, e^{j\frac{2\pi d}{\lambda}u}, \dots, e^{j\frac{2\pi d}{\lambda}(N_x-1)u}]^T$  and  $\mathbf{p}(v) = [1, e^{j\frac{2\pi d}{\lambda}v}, \dots, e^{j\frac{2\pi d}{\lambda}(N_y-1)v}]^T$ , for  $i \in \{\text{RIS}, \text{BS}\}$ . Going through the same derivation,  $\mathbf{H}$  is expressed as

$$\mathbf{H} = \sum_{l=1}^{L_h} z_{h,l} \mathbf{a}_{\text{M}_{\text{UE}}}(\theta_{h,l}^U, \varphi_{h,l}^U) \mathbf{a}_{\text{M}_{\text{RIS}}}^H(\theta_{h,l}^R, \varphi_{h,l}^R), \quad (8)$$

$$= \mathbf{A}_{\text{M}_{\text{UE}}}(\Psi_U) \text{diag}(\mathbf{z}_h) \mathbf{A}_{\text{M}_{\text{RIS}}}^H(\Psi_R),$$

where  $\Psi_U = [(\theta_{h,1}^U, \varphi_{h,1}^U), (\theta_{h,2}^U, \varphi_{h,2}^U), \dots, (\theta_{h,L_h}^U, \varphi_{h,L_h}^U)]^T$ ,  $\Psi_R = [(\theta_{h,1}^R, \varphi_{h,1}^R), (\theta_{h,2}^R, \varphi_{h,2}^R), \dots, (\theta_{h,L_h}^R, \varphi_{h,L_h}^R)]$ , and  $\mathbf{z}_h = [z_{h,1}, z_{h,2}, \dots, z_{h,L_h}]^T$ . The overall channel  $\mathbf{H}_{\text{eff}} \in \mathbb{C}^{M_{\text{UE}} \times M_{\text{BS}}}$  between the BS-RIS-UE is written as

$$\mathbf{H}_{\text{eff}} = \beta(d_g, d_h, \theta_{des}, \varphi_{des}) \mathbf{H} \mathbf{O} \mathbf{G}, \quad (9)$$

where  $\beta(d_g, d_h, \theta_{des}, \varphi_{des})$  is the total path loss given by (3).

#### IV. RIS CONTROL

This section describes how to control the reflecting coefficients of the RIS so that all manipulation (beamforming/steering) can occur in real-time. The authors in [15] developed a path loss model proved analytically and experimentally. The optimal phases to beamform/steer a reflected signal in a predefined direction is represented in (4), and it can be expressed as

$$\text{vec}(\phi) = \Lambda_x(\theta_t, \varphi_t, \theta_{des}, \varphi_{des}) \otimes \Lambda_y(\theta_t, \varphi_t, \theta_{des}, \varphi_{des}), \quad (10)$$

where  $\Lambda_x(\cdot)$  and  $\Lambda_y(\cdot)$  can be viewed as steering vectors on the elevation and the azimuth direction, respectively, with

$$\Lambda_x = [e^{j\frac{-N_{\text{RIS}}}{2} \frac{2\pi}{\lambda} d_x(\Gamma_x)}, \dots, e^{j\frac{N_{\text{RIS}}}{2} \frac{2\pi}{\lambda} d_x(\Gamma_x)}]^T, \quad (11)$$

and

$$\Lambda_y = [e^{j\frac{-N_{\text{RIS}}}{2} \frac{2\pi}{\lambda} d_y(\Gamma_y)}, \dots, e^{j\frac{N_{\text{RIS}}}{2} \frac{2\pi}{\lambda} d_y(\Gamma_y)}]^T, \quad (12)$$

where  $\Gamma_x = \sin \theta_t \cos \varphi_t + \sin \theta_{des} \cos \varphi_{des}$  and  $\Gamma_y = \sin \theta_t \sin \varphi_t + \sin \theta_{des} \sin \varphi_{des}$ .

For simplicity, we consider the case with maximum power accumulated i.e.,  $\theta_t \approx 0$  where the received beam is perpendicular to RIS surface, then (10) becomes a function of the destination angles only.

$$\text{vec}(\phi) = \Lambda_x(\theta_{des}, \varphi_{des}) \otimes \Lambda_y(\theta_{des}, \varphi_{des}). \quad (13)$$

As we can see, the reflection coefficients of RIS are equivalent to the steering vector of a UPA [29] in the MIMO model. To adjust the beam direction of the RIS, we just need to



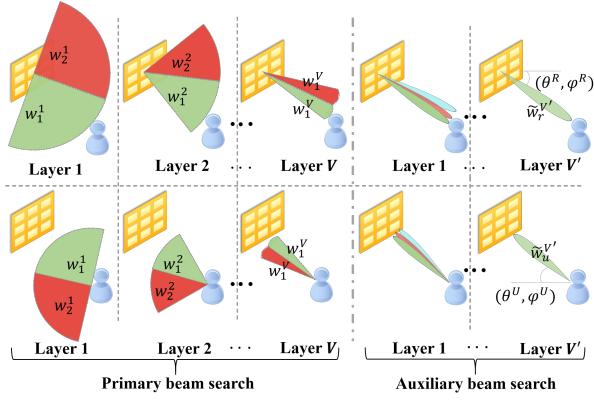


Fig. 3: Hierarchical beam searching algorithm procedures for channel estimation.

multiply  $\phi$  with a weight vector which is designed to steer the RIS elements array toward the desired direction. According to (13), the array factor of an RIS is given as

$$AF_{\text{RIS}} = \sum_{n=-N_{\text{RIS}}/2}^{N_{\text{RIS}}/2} \sum_{m=-N_{\text{RIS}}/2}^{N_{\text{RIS}}/2} w_{m,n}, \quad (14)$$

where  $w_{m,n} = e^{j[m\frac{2\pi}{\lambda}d_x(\Gamma_x) + n\frac{2\pi}{\lambda}d_y(\Gamma_y)]}$  denotes the weight vector.

## V. PROPOSED CHANNEL ESTIMATION

In order to apply the proposed estimation technique, the effective channel in (9) can be rewritten as

$$\mathbf{H}_{\text{eff}} = \beta(d_g, d_h, \theta_{des}, \varphi_{des}) \hat{\mathbf{H}} \hat{\mathbf{\Theta}} \hat{\mathbf{G}}, \quad (15)$$

where  $\hat{\mathbf{H}} = \mathbf{A}_{MUE}(\Psi_U) \text{diag}(\mathbf{z}) \mathbf{A}_{MIRS}^H(\Psi_R)$  and  $\hat{\mathbf{G}} = \mathbf{A}_{MIRS}(\Omega_R) \text{diag}(e^{j\angle \mathbf{z}_g}) \mathbf{A}_{MBS}^H(\Omega_B)$ , and  $\mathbf{z}$  is the gain of the cascaded channel  $\mathbf{G}$  and  $\mathbf{H}$  is considered. Since  $\mathbf{G}$  is directly responsible of altering the RIS phases, it is more meaningful to represent it only in terms of  $\angle \mathbf{z}_g$ , and include the channel gain  $|\mathbf{z}_g|$  into  $\mathbf{H}$ . Writing the channel in this form allows us to estimate  $\hat{\mathbf{H}}$  and  $\hat{\mathbf{G}}$  separately.

### A. Estimating BS-RIS channel

Since mmWave channel is sparse and the new representation of channel BS-RIS has unit amplitude, the problem of estimating  $\hat{\mathbf{G}}$  becomes equivalent to the estimation of  $(e^{j\angle \mathbf{z}_g})$  of each path. From Section II-B,  $\hat{\mathbf{G}}$  causes a shift in the reflected beam, and hence, estimating this shift leads to estimate  $\hat{\mathbf{G}}$  itself. This could be done in three steps. First, estimating AoA and AoD for the RIS reflected signal. Next, substituting these angles in (14) to get the reflection coefficients of RIS in the absence of  $\hat{\mathbf{G}}$ 's effect. Then, these coefficients are compared to the last coefficient set by the BS, and subtracted from each other to get  $\hat{\mathbf{G}}$ .

1) *Finding AoA and AoD*: An exhaustive beam searching algorithm can be used in this case, where all possible angles are tested to find one optimal AoA/AoD. However, this approach requires a large amount of time due to its complexity [30]. Thus, we adopt a two-stage beam training

method depicted in Fig. 3 consisting of primary and secondary beam search [31]. For simplicity, the training procedure is described in azimuth only in the latter part of this subsection, and by using the same analogy the procedure in elevation can be deduced.

The primary search will use hierarchical search to reduce the search time. As given in [31], two-way tree stage search is used here at each layer. Let  $w_n^l$  denotes the codeword of the  $n^{\text{th}}$  beam vector at the  $l^{\text{th}}$  layer, at each layer only  $2^l$  antennas are activated. In total, there will be  $\aleph$  possible beams and  $V = \log_2(\aleph)$  layers, where each parent codeword  $w_n^l$  has two child codewords  $w_n^{l+1}$  and  $w_{n+1}^{l+1}$ . It is aimed to obtain  $(\theta_{h,l}^U, \varphi_{h,l}^U)$  and  $(\theta_{h,l}^R, \varphi_{h,l}^R)$  through multiple steps. Starting by testing four wide-beams in four successive time slots, where the RIS uses  $\mathbf{w}_r = [w_1^1, w_2^1]$  at reflecting mode<sup>2</sup> and the UE uses  $\mathbf{w}_u = [w_1^1, w_2^1]$  at the receiving mode. The resulted signal from the  $l^{\text{th}}$  stage can be written as

$$\mathbf{y}^l = \beta(d_g, d_h, \theta_{des}, \varphi_{des}) \mathbf{w}_u^H \hat{\mathbf{H}} \mathbf{w}_r \hat{\mathbf{s}} + \mathbf{w}_u^H \mathbf{n}, \quad (16)$$

where  $\hat{\mathbf{s}} = \hat{\mathbf{G}}\mathbf{s}$ ,  $\mathbf{s} = [s_1, s_2, \dots, s_Z]^T$  is  $Z \times 1$  vector of transmitted symbols, and  $\mathbf{n}$  is  $Z \times 1$  complex Gaussian noise vector with zero-mean and variance  $\sigma_o^2$ . At each stage we search for the pair  $(\tilde{\mathbf{w}}_r^l, \tilde{\mathbf{w}}_u^l)$  that satisfies the highest received signal-to-noise ratio (SNR), i.e.,

$$\max_{\mathbf{w}_r, \mathbf{w}_u} \left( \left| \mathbf{w}_u^H \hat{\mathbf{H}} \mathbf{w}_r \hat{\mathbf{s}} \right|^2 \right) = \left| (\tilde{\mathbf{w}}_u^l)^H \hat{\mathbf{H}} \tilde{\mathbf{w}}_r^l \right|^2. \quad (17)$$

After  $V$  beam search, the optimum pair  $(\tilde{\mathbf{w}}_r^V, \tilde{\mathbf{w}}_u^V)$  is obtained. The elements of the primarily codebook matrix in azimuth of  $K$  beam patterns,  $\tau$  discrete phase shift, and  $N_{\text{RIS}}$  elements is given by [31]

$$w_{n,k}^{az} = \exp \left( -j \frac{2\pi}{\tau} \left\lfloor \frac{nk\tau}{K} \right\rfloor \right), \quad (18)$$

where  $n = 0, 1, \dots, N_{\text{RIS}} - 1$  and  $k = 0, 1, \dots, K - 1$ . This codebook ensures that it has  $\aleph$  possible states, and it fully spans the azimuth range. Similarly, the primary beam codebook matrix in elevation is given by

$$w_{n,k}^{el} = \exp \left( -j \frac{2\pi}{\tau} \left\lfloor \frac{nk\tau}{2K-2} \right\rfloor \right). \quad (19)$$

Second stage starts after acquiring the primary codebook, where we make a secondary beam search by rotating the primary beam to create higher-resolution secondary beams. These beams define the auxiliary codebook. Finally,  $(\tilde{\mathbf{w}}_r, \tilde{\mathbf{w}}_u)$  is considered the optimum codebook.

Since the optimal transmission beam is represented by a weighting vector  $\mathbf{w} = \tilde{\mathbf{w}}^{el} \otimes \tilde{\mathbf{w}}^{az}$ , both AoA/AoD can be obtained. The AoA from RIS to UE can be found as

$$(\theta_{h,l}^U, \varphi_{h,l}^U) = \left( \sin^{-1} \left( \frac{-\lambda}{\tau} \left\lfloor \frac{k\tau}{K} \right\rfloor \right), \sin^{-1} \left( \frac{-\lambda}{\tau} \left\lfloor \frac{k\tau}{2K-2} \right\rfloor \right) \right). \quad (20)$$

In our model, since the RIS is located near to UE, we assume that the antenna arrays of the UE is always parallel to the RIS, hence  $(\theta_{h,l}^R, \varphi_{h,l}^R) = (\theta_{h,l}^U, \varphi_{h,l}^U)$  [32].

<sup>2</sup>Note that by setting the phases of the RIS according to equation (14), and setting the weighting vector to be any chosen codeword i.e.,  $\mathbf{w} = (\mathbf{w}_r^{el} \otimes \mathbf{w}_r^{az})$ , beam searching could be implemented at the RIS.

2) *Estimating  $\hat{\mathbf{G}}$* : If the RIS phases are set to direct the beam of the reflected signal toward the UE's location  $(\theta_{h,l}^R, \varphi_{h,l}^R)$ , then the beam would be distorted and the radiation is shifted toward different direction due to the effect of channel  $\hat{\mathbf{G}}$ . Mathematically, this could be expressed as

$$\hat{\mathbf{H}}\Theta^V\hat{\mathbf{G}} = \hat{\mathbf{H}}\Theta(\theta_{h,l}^R, \varphi_{h,l}^R)\mathbf{G}_{opt}, \quad (21)$$

where  $\mathbf{G}_{opt} = \mathbf{G}(\theta_{g,1}^B, \varphi_{g,1}^B, \theta_{g,1}^R, \varphi_{g,1}^R)$ <sup>3</sup>, and  $\Theta^V$  is the last configured set of phases by the BS at the  $V$ -th stage of beam searching process. By exploiting the angles obtained from (20) and by substituting them in (13),  $\hat{\mathbf{G}}$  can be estimated directly as

$$\hat{\mathbf{G}} = (\Theta^V)^{-1}\Theta(\theta_{h,l}^R, \varphi_{h,l}^R)\mathbf{G}_{opt}. \quad (22)$$

By adopting this design, we assure that the effect of  $\hat{\mathbf{G}}$  is known and its effects are cancelled by the RIS. Therefore, to set communication with any UE at direction  $(\theta_{des}, \varphi_{des})$  throughout the RIS, we simply set the phases by

$$\Theta = \Theta(\theta_{des}, \varphi_{des})\mathbf{G}_{opt}\hat{\mathbf{G}}^H(\hat{\mathbf{G}}\hat{\mathbf{G}}^H)^{-1}. \quad (23)$$

Please refer to Appendix. A

By substituting (23) in the total channel we obtain

$$\hat{\mathbf{H}}\Theta\hat{\mathbf{G}} = \hat{\mathbf{H}}\Theta(\theta_{des}, \varphi_{des})\mathbf{G}_{opt}, \quad (24)$$

where  $\Theta(\theta_{des}, \varphi_{des})$  is set for any desired location, and the channel estimation problem is reduced to estimate  $\hat{\mathbf{H}}$  only which will be explained in the next subsection.

### B. Estimating RIS-UE channel

Without loss of generality, assuming one RF chain is activated at the BS side and  $Z$  symbols are transmitted, channel estimation model given in [21] is adopted here to estimate path gains of all paths. For that, the system model is given as

$$\mathbf{y} = \mathbf{Q}^H\mathbf{H}_{eff}\mathbf{F}\mathbf{s} + \mathbf{Q}^H\mathbf{n}, \quad (25)$$

where  $\mathbf{y} \in \mathbb{C}^{Z \times 1}$  is the received signal at UE, and  $\mathbf{Q} \in \mathbb{C}^{M_{UE} \times Z}$  and  $\mathbf{F} \in \mathbb{C}^{M_{BS} \times Z}$  are the hybrid combining and the precoder matrices, respectively. The received signal at the UE can be explicitly expressed as

$$\mathbf{y} = \beta(d_g, d_h, \theta_{des}, \varphi_{des})\mathbf{Q}^H\hat{\mathbf{H}}\Theta\hat{\mathbf{G}}\mathbf{F}\mathbf{s} + \mathbf{Q}^H\mathbf{n}. \quad (26)$$

Assuming  $\mathbf{x} = \Theta\hat{\mathbf{G}}\mathbf{F}\mathbf{s} \in \mathbb{C}^{M_{RIS} \times 1}$ , where each element  $x_i$  is the transmitted symbol. For channel estimation, we will transmit known symbols at known indices, each received signal corresponding to a transmitted pilot symbol at  $u$  time slot is given as

$$y_{p,u} = \beta(d_g, d_h, \theta_{des}, \varphi_{des})\mathbf{q}_u^H\hat{\mathbf{H}}\mathbf{x}_{p,u} + \mathbf{q}_u^H\mathbf{n}_{p,u}. \quad (27)$$

Within  $U$  time slots,  $U_p$  different pilot sequences are sent in each time slot, and  $\mathbf{y}_p = \beta(d_g, d_h, \theta_{des}, \varphi_{des})\mathbf{Q}^H\hat{\mathbf{H}}\mathbf{x}_p + \mathbf{Q}^H\mathbf{n}_p$ , where  $\mathbf{y}_p = [y_{p,1}, y_{p,2}, \dots, y_{p,U}]^T$  and  $\mathbf{Q} = [\mathbf{q}_1, \mathbf{q}_2, \dots, \mathbf{q}_U]^T$ . By setting  $\mathbf{Y} = [\mathbf{y}_1, \mathbf{y}_2, \dots, \mathbf{y}_p, \dots, \mathbf{y}_{U_p}]^T$ ,  $\mathbf{X} = [\mathbf{x}_1, \mathbf{x}_2, \dots, \mathbf{x}_{U_p}]^T$  and  $\mathbf{N} = [\mathbf{n}_1, \mathbf{n}_2, \dots, \mathbf{n}_{U_p}]^T$ , we get

$$\mathbf{Y} = \mathbf{Q}^H\hat{\mathbf{H}}\mathbf{X} + \mathbf{Q}^H\mathbf{N}. \quad (28)$$

<sup>3</sup>Note that the angles  $\theta_{g,1}^B, \varphi_{g,1}^B, \theta_{g,1}^R, \varphi_{g,1}^R$  are known from the fixed geometry of the deployment of RIS and BS.

Using the fact that the mmWave channel is sparse, the estimation of the channel  $\hat{\mathbf{H}}$  become equivalent to the estimation of  $\mathbf{z}$ ,  $\Psi_U$  and  $\Psi_R$ , and the problem is formulated as

$$\min_{\mathbf{z}, \Psi_U, \Psi_R} P_1(\mathbf{z}, \Psi_U, \Psi_R) \triangleq \|\hat{\mathbf{z}}\|_0, s.t. \|\mathbf{Y} - \mathbf{Q}^H\hat{\mathbf{H}}\mathbf{X}\|_F \leq \epsilon, \quad (29)$$

where  $\|\hat{\mathbf{z}}\|_0$  represents the number of non-zero elements, i.e., the sparsest solution of the sparse channel  $\hat{\mathbf{H}}$ ,  $\hat{\mathbf{H}}$  is the estimated channel matrix for  $\hat{\mathbf{H}}$ , and  $\epsilon$  is the estimation error tolerance.

Since the log-sum penalty is more sparsity encouraging, the log-norm instead of  $\|\hat{\mathbf{z}}\|_0$  can be used here [33]. In addition, both  $\Psi_U, \Psi_R$  are already obtained in Section V-A using the beam searching algorithm, thus the optimization is performed according to  $\mathbf{z}$  only, and the problem  $P_1$  is given as

$$\min_{\mathbf{z}} P_2(\mathbf{z}) \triangleq \sum_{l=1}^{L_h} \log(|\hat{\mathbf{z}}|^2 + \delta), s.t. \|\mathbf{Y} - \mathbf{Q}^H\hat{\mathbf{H}}\mathbf{X}\|_F \leq \epsilon, \quad (30)$$

where  $\delta$  ensures that the logarithmic function is always in its domain of definition. In addition to minimizing the number of paths, minimizing the channel estimation error is needed. Hence, a regularization parameter  $\zeta > 0$  is added, and  $P_2$  is reshaped to the following optimization problem

$$\min_{\mathbf{z}} P_3(\mathbf{z}) \triangleq \sum_{l=1}^{L_h} \log(|\hat{\mathbf{z}}|^2 + \delta) + \zeta \|\mathbf{Y} - \mathbf{Q}^H\hat{\mathbf{H}}\mathbf{X}\|_F^2. \quad (31)$$

It turned out that the minimization of  $P_3$  is equivalent to the minimization of the iterative surrogate function [33]

$$\min_{\mathbf{z}} P_4^{(i)}(\mathbf{z}) \triangleq \zeta^{-1}\mathbf{z}^H\mathbf{D}^{(i)}\mathbf{z} + \|\mathbf{Y} - \mathbf{Q}^H\hat{\mathbf{H}}\mathbf{X}\|_F^2, \quad (32)$$

where  $\mathbf{D}^{(i)}$  is expressed as

$$\mathbf{D}^{(i)} = \text{diag} \left( \frac{1}{|\hat{z}_1^{(i)}|^2 + \delta}, \frac{1}{|\hat{z}_2^{(i)}|^2 + \delta}, \dots, \frac{1}{|\hat{z}_{L_h}^{(i)}|^2 + \delta} \right), \quad (33)$$

and  $\hat{\mathbf{z}}^{(i)}$  is the estimate of  $\mathbf{z}$  at the  $i$ th iteration. Then, the optimization of (32) becomes as follows

$$P_4^{(i)}(\mathbf{z}) = \zeta^{-1}\mathbf{z}^H\mathbf{D}^{(i)}\mathbf{z} + \sum_{p=1}^{U_p} \|\mathbf{y}_p - \mathbf{T}_p\mathbf{z}\|_2^2, \quad (34)$$

where  $\mathbf{T}_p = \mathbf{Q}^H\mathbf{A}_{MUE}(\Psi_U)\mathbf{A}_{MIRS}^H(\Psi_R)\mathbf{x}_p$ .

$$\begin{aligned} P_4^{(i)}(\mathbf{z}) &= \zeta^{-1}\mathbf{z}^H\mathbf{D}^{(i)}\mathbf{z} + \sum_{p=1}^{U_p} (\mathbf{y}_p - \mathbf{T}_p\mathbf{z})^H(\mathbf{y}_p - \mathbf{T}_p\mathbf{z}) \\ &= \mathbf{z}^H \left( \zeta^{-1}\mathbf{D}^{(i)} + \sum_{p=1}^{U_p} \mathbf{T}_p^H\mathbf{T}_p \right) \mathbf{z} - \mathbf{z}^H \left( \sum_{p=1}^{U_p} \mathbf{T}_p^H\mathbf{y}_p \right) \\ &\quad - \left( \sum_{p=1}^{U_p} \mathbf{y}_p^H\mathbf{T}_p \right) \mathbf{z} + \left( \sum_{p=1}^{U_p} \mathbf{y}_p^H\mathbf{y}_p \right). \end{aligned} \quad (35)$$

For optimizing (35), the next step is obtained

$$\frac{\partial P_4^{(i)}(\mathbf{z})}{\partial \mathbf{z}} = \mathbf{z}^H \left( \zeta^{-1}\mathbf{D}^{(i)} + \sum_{p=1}^{U_p} \mathbf{T}_p^H\mathbf{T}_p \right) - \left( \sum_{p=1}^{U_p} \mathbf{y}_p^H\mathbf{T}_p \right) = 0. \quad (36)$$

Therefore, the optimal  $\hat{\mathbf{z}}$  that corresponds to the best estimation of  $\hat{\mathbf{H}}$  at the  $i$ th iteration is given by

$$\begin{aligned} \mathbf{z}_{opt}^{(i)} &\triangleq \left( \zeta^{-1} \mathbf{D}^{(i)} + \sum_{p=1}^{U_p} \mathbf{T}_p^H \mathbf{T}_p \right)^{-1} \left( \sum_{p=1}^{U_p} \mathbf{T}_p^H \mathbf{y}_p \right) \\ &\triangleq \left( \zeta^{-1} \mathbf{D}^{(i)} + \sum_{p=1}^{U_p} \mathbf{T}_p^H \mathbf{T}_p \right) \left( \sum_{p=1}^{U_p} \mathbf{y}_p^H \mathbf{T}_p \right)^{-1}. \end{aligned} \quad (37)$$

In this iterative method,  $\zeta$  is designed to be adaptive to fit both a sparser estimation and a fast search. It is investigated in details in [21], [33].

---

**Algorithm 1:** The proposed three-stage RIS channel framework

---

```

1 Estimating BS-RIS channel  $\mathbf{G}$ :
2   Finding AoA/AoD between RIS-UE():
3   |   Primary beam search ( $w_n^V, w_{n+1}^V$ )
4   |   Auxiliary beam search ( $\hat{\mathbf{w}}_r, \hat{\mathbf{w}}_u$ )
5   |   Output:  $\Theta^{V'}, \theta_{h,l}^R, \varphi_{h,l}^R$ 
6   Estimation of  $\hat{\mathbf{G}}(\Theta^{V'}, \theta_{h,l}^R, \varphi_{h,l}^R)$ :
7   |    $\hat{\mathbf{G}} = (\Theta^{V'})^{-1} \Theta(\theta_{h,l}^R, \varphi_{h,l}^R) \mathbf{G}_{opt}$ 
7 Estimating RIS-UE channel  $\mathbf{H}$ :
8   Input: Received signal  $Y$ , pilots signals  $X$ ,
9   combining matrix  $W$ ,  $\Psi_U$ ,  $\Psi_R$ , pruning
10  threshold  $z_{th}$  and termination threshold  $\epsilon_{th}$ .
11  Output: Path gain of all paths.
12  Initiate  $\hat{\mathbf{z}}^{(0)} = \hat{\mathbf{z}}_{opt} = (\Psi_R, \Psi_U)$  according to (37).
13  while  $\|\hat{\mathbf{z}}^{(i+1)} - \hat{\mathbf{z}}^{(i)}\| < \epsilon_{th}$  do
14  |   Update  $\zeta$ .
15  |   Estimate the path gains  $\hat{\mathbf{z}}^{(i+1)}$  according to
16  |   (37).
17  |   Prune path  $l_h$  if  $\hat{\mathbf{z}}^{(i+1)} < \hat{\mathbf{z}}^{(i)}$ .
18  |    $\hat{\mathbf{z}} = \hat{\mathbf{z}}^{(last)}$ .
19  |    $\hat{\mathbf{H}} = \mathbf{A}_{MUE}(\Psi_U) \text{diag}(\mathbf{z}) \mathbf{A}_{MRS}^H(\Psi_R)$ .
15 Tracking channel  $\mathbf{H}$  parameters ( $z, \theta, \varphi$ ):
16  Input: the estimated parameters:  $\mathbf{z}_{opt}$ ,  $\theta$ , and  $\varphi$ .
17  Update the parameters using EKF algorithm.
18  Update the phases
19  |    $\Theta = \Theta(\theta, \varphi) \mathbf{G}_{opt} \hat{\mathbf{G}}^H (\hat{\mathbf{G}} \hat{\mathbf{G}}^H)^{-1}$ 
20  Track the observation signal using (38).
21  Repeat lines 16-18 till next estimation.
```

---

### C. Channel Tracking

After estimating the channel parameters, i.e., channel coefficients, AoA, and AoD, and since the UE is under mobility assumption, a channel tracking approach has been introduced here to avoid often channel estimation by tracking the channel parameters. The channel tracking algorithms are significantly fast, reliable, and robust which allow efficient data transfer between transmitters and receivers in mmWave communications. Channel tracking in mmWave systems is firstly presented in [34], where an EKF based tracking algorithm is proposed to

track AoA/AoD while the channel coefficient remains constant. However, the method has difficulties to track in a fast-changing channel environment since it requires pre-requisites for a full scan that causes long time measurement. To decrease the measurement time and provide a more suitable tracking algorithm, the authors in [35] proposed an alternative solution that requires only a single measurement with EKF estimation and a beam switching design. Additionally, least mean square (LMS) and bi-directional LMS (BiLMS) algorithms are introduced in [36] where advantages of both algorithms are presented compared to EKF algorithm on imperfect CSI conditions while having faster convergence characteristics as SNR increases. However, both algorithms are not suitable for higher nonlinearity systems. Therefore, the EKF tracking algorithm is used in our RIS-assisted framework due to its low complexity and good tracking performance.

The tracking algorithm starts with setting a pair of transmitting and receive beams according to the estimated elevation and azimuth AoA/AoD from the channel estimator. One main point that should be taken into consideration is that while tracking, the predicted channel parameters should stay close to the actual values so that the UE stays within half of the beamwidth. Otherwise, if the tracking is no longer reliable or the path of the beams does not exist anymore, the channel parameters should be re-estimated.

The discrete-time model for the received signal symbol period at UE side is given in (26). Assuming that each vector in  $\mathbf{F}$  is given by  $\mathbf{f} = \mathbf{a}_{MBS}(\theta, \varphi)$  for the LoS path. In order to start the tracking process, the measurement function should be known. From (26), the measurement function is used to track the observation signal and can be given as

$$\mathbf{g}_{\text{measure}} = \beta(d_g, d_h, \theta_{des}, \varphi_{des}) \mathbf{Q}^H \hat{\mathbf{H}} \Theta \hat{\mathbf{G}} \mathbf{F}, \quad (38)$$

where  $\mathbf{g}_{\text{measure}}$  depends on the channel parameters including path coefficients, elevation and azimuth AoD/AoA angles from both channels; BS-RIS and RIS-UE. EKF algorithm [35] is used to track these parameters. To evaluate the performance of the tracking process, a state evolution model is needed for the tracked parameters. A first-order Gaussian-Markov model is adopted for the path coefficient evolution over the time, while a Gaussian process noise model is assumed for the elevation and azimuth AoD/AoA [32], [35], [36].

The proposed three-stage RIS framework is summarized in Algorithm 1.

## VI. SIMULATION RESULTS

In this section, simulation results are presented to evaluate the performance of the proposed RIS-assisted framework. The simulation parameters are provided in Table II.

### A. Channel Estimation Performance

At the first step of the proposed framework, we implement a two-stage beam search algorithm to determine the UE's location i.e., the AoD/AoA in elevation and azimuth domains. Fig. 4 illustrates the primary beam patterns reflected from the RIS, where  $N_{RIS} = 8$  elements, each elements can perform 5 discrete phases shifts, and the resolution achieves



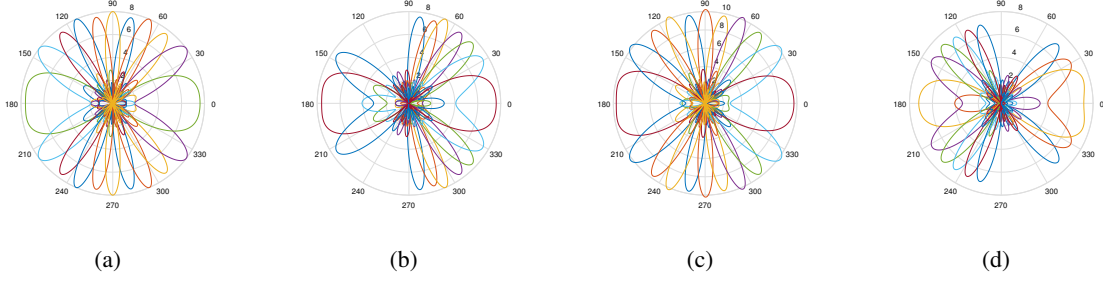


Fig. 4: Primary beam patterns  $N_{RIS} = 8$ ,  $\tau = 5$ ,  $K = 10$  when channel  $\mathbf{G}$  is ideal in (a) azimuth and (b) elevation domains, and when channel  $\mathbf{G}$  is geometric model with  $L_g = 5$  paths in (c) azimuth and (d) elevation domains.

TABLE II: Simulation Configuration

Parameters	Value
Operating frequency $f_c$	28 GHz
Channel paths $L_g$	5
Channel paths $L_h$	1
Antenna array size at BS $M_{BS}$	256
Distance between antenna elements $d$	$\lambda/2$
Number of beam pattern in the codebook $K$	10
Estimation error tolerance $\epsilon$	$1e-8$

$K = 10$  different patterns. Fig. 4a and Fig. 4b illustrate the ten different patterns used at the final stage in elevation and azimuth, respectively. It should be mentioned that even though channel  $\mathbf{G}$  will shift the reflected beam corresponding to each codeword as discussed in Subsection II-B, still the resulted shifted beams will scan the whole space. This is shown by Fig. 4c and Fig. 4d, where we can see that the channel  $\mathbf{G}$  just caused a rotation in total beam patterns of the codebook. However, the UE will use the codebook normally and based on the received optimal codeword, it can find the AoA by just comparing this codeword to a predefined table, or from the polar diagram illustrated in Fig. 4a and Fig. 4b.

In the second step, channel  $\mathbf{H}$  is estimated using the iterative resolution algorithm and the performance of this algorithm is evaluated using normalized mean square error (NMSE) given by

$$\text{NMSE} = \mathbb{E} \left[ \frac{\|\tilde{\mathbf{H}} - \hat{\mathbf{H}}\|_F^2}{\|\hat{\mathbf{H}}\|_F^2} \right]. \quad (39)$$

We consider narrowband mmWave channel with a MIMO system, number of antennas at the base station and at UE is  $N_{BS} = 16 \times 16 = 256$  and  $N_{UE} = 2 \times 2 = 4$ , respectively. The path gains are assumed to have Gaussian distribution. RIS is assumed to have different geometries  $M_{RIS} = 4 \times 4 = 16$ ,  $M_{RIS} = 8 \times 8 = 64$  and  $M_{RIS} = 16 \times 16 = 256$ , for each case number of pilots is  $U_p = 8$ ,  $U_p = 32$  and  $U_p = 128$ , respectively. We also assume one dominant LoS path  $L_h = 1$  between RIS-UE. Conventional methods i.e., cascaded channel estimation, were adopted in our system to be compared with the proposed algorithm, and most importantly no prior knowledge of the UE's location is assumed.

Fig. 5 compares the NMSE performance against SNR. The proposed scheme achieves very high performance compared the the conventional ones, where the NMSE keeps decreasing

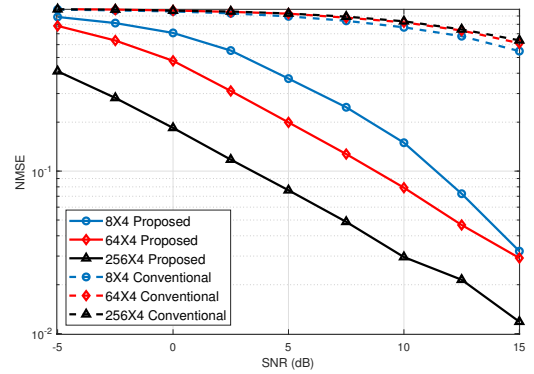


Fig. 5: NMSE performance comparison between the proposed framework and conventional approaches of channel  $\mathbf{H}$  at different RIS array sizes.

with the SNR increasing, reaching almost 0.01 normalized error at  $\text{SNR} = 15$  dB and  $M_{RIS} = 256$ . The reason is that in the proposed scheme, the power is focused on the target UE before starting channel estimation protocol, this result is also reflected in the same figure at low SNR values, where NMSE is still relatively small even though the transmit power is minimal. Also, increasing the number RIS elements gives the better channel estimation, where the lowest NMSE corresponded to  $M_{RIS} = 256$ , then  $M_{RIS} = 64$ , and lastly to  $M_{RIS} = 16$ . However, the conventional algorithms, regardless of the number of RIS elements, have very bad NMSE performance through all SNR values. The reason is that the energy is not beamformed toward the UE most of the time, and the received power from the beam sides is always weak, and thus the channel cannot be estimated reliably. The slight change at high SNR indicates that the UE in this case is receiving slightly higher power, but still it is not enough because it does not directly come from the main beam.

### B. The Channel Tracking Performance

In this subsection, we assume that the channel between the BS and RIS is fixed and its parameters are constant during the tracking period. Also, it is assumed that the channel remains stationary during this observation interval, and the channel sparsity in the mmWave makes the paths to be likely separated

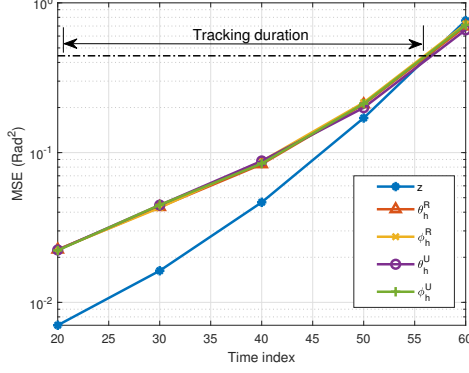


Fig. 6: MSE of the tracked parameters: complex path coefficient, elevation and azimuth AoDs from the RIS, and elevation and azimuth AoAs at UE using EKF tracking algorithm.

from each other under the assumption that the RIS is located near to UE location. Hence, only one single path falls into the main beam direction  $L_h = 1$  [35], giving that the state space vector at each time index is

$$\mathbf{x}_{state} = [z_{\Re} \ z_{\Im} \ \theta_h^R \ \varphi_h^R \ \theta_h^U \ \varphi_h^U]^T, \quad (40)$$

where  $z = z_{\Re} + jz_{\Im}$ . By using the real and imaginary part of  $z$ , the state vector  $\mathbf{x}_{state}$  is a real vector which helps to avoid implementation issues when real and complex numbers are combined. Fig. 6 shows the MSE of the tracked channel parameters between RIS and UE using EKF algorithm with the same filter setups as in [35] at SNR= 20 dB. It is clearly shown that the algorithm has the ability to reduce the estimation overhead for longer time since it can keep the error below a certain threshold of half power beamwidth where it is given as  $\Delta\theta_{3dB} \approx \frac{\lambda}{\sqrt{M_{RISd}}} 0.886$  [37].

The overall performance of the proposed three-stage RIS framework is illustrated in Fig. 7, where it is assumed that both proposed and conventional RIS-assisted communication channel estimation techniques know the location of the UE at the initial state, and that they are beamforming toward this direction at SNR= 20 dB. This assumption is favorable to the conventional scheme. The simulation consists of three states, in which the UE is stationary at first, then it starts moving and finally becomes stationary again. Fig. 7 shows that at the initial state both methods perform well, achieving low normalized error. However, the performance totally changes as the UE moves. In the proposed channel estimation scheme, as the UE starts moving, the channel is tracked until a certain threshold and the beamforming is shifted based on the tracked parameters. After that, channel estimation is needed where the result converges again to a minimum NMSE. In case of the conventional method, the error increases very fast which needs to be compensated by estimating the channel where the result settles to NMSE = 0.5, resulting in a huge performance gap between the two schemes.

## VII. CONCLUSION

In this paper, we propose a three-stage framework for an RIS-aided mmWave MIMO communication system. In the

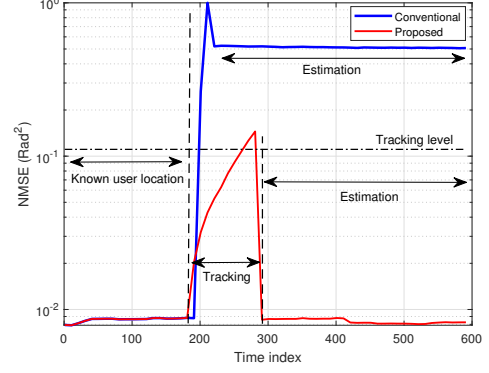


Fig. 7: The overall system performance for the proposed three-stage RIS framework compared to conventional cascaded channel estimation methods.

first and the second stages, the channel estimation problem is extensively studied and new approach is proposed to estimate BS-RIS channel (channel  $\mathbf{G}$ ) and RIS-UE channel (channel  $\mathbf{H}$ ) separately, by exploiting the shift in the direction of the beams reflected from RIS due to  $\mathbf{G}$  effect. The estimation of channel  $\mathbf{G}$  is used to develop a low-complex, real-time applicable phase design. Then, the channel  $\mathbf{H}$  is estimated using the iterative resolution method and the prior knowledge of AoD/AoA that were estimated in the previous step. In the third stage, channel tracking algorithms are applied to track the channel between RIS and UE, since estimating channels  $\mathbf{G}$  and  $\mathbf{H}$  are done separately which allows the user to have some level of mobility. The performance analysis showed that the proposed framework can provide an accurate channel estimation. The proposed framework for RIS-aided communication was developed under very practical assumptions which makes it very useful to be implemented with the available RIS prototypes such MITs **RFocus prototype** [38], that beamforms and focuses the impinging radio waves towards specified direction and location, respectively.

## ACKNOWLEDGMENT

This work was supported by the Scientific and Technological Research Council of Turkey under Grant No. 5200030.

## APPENDIX A PROOF OF EQUATION (23)

To cancel the effect of channel  $\hat{\mathbf{G}}$ , the outcome of the effective channel should be given as

$$\hat{\mathbf{H}}\hat{\mathbf{\Theta}}\hat{\mathbf{G}} = \hat{\mathbf{H}}\hat{\mathbf{\Theta}}(\theta_{des}, \varphi_{des})\mathbf{G}_{opt}, \quad (41)$$

which is equivalent to  $\hat{\mathbf{\Theta}}\hat{\mathbf{G}} = \hat{\mathbf{\Theta}}(\theta_{des}, \varphi_{des})\mathbf{G}_{opt}$ . Then we find

$$\begin{aligned} \hat{\mathbf{\Theta}}\hat{\mathbf{G}} &= \hat{\mathbf{\Theta}}(\theta_{des}, \varphi_{des})\mathbf{G}_{opt} \\ \hat{\mathbf{\Theta}}\hat{\mathbf{G}}\hat{\mathbf{G}}^H &= \hat{\mathbf{\Theta}}(\theta_{des}, \varphi_{des})\mathbf{G}_{opt}\hat{\mathbf{G}}^H \\ \hat{\mathbf{\Theta}}(\hat{\mathbf{G}}\hat{\mathbf{G}}^H)(\hat{\mathbf{G}}\hat{\mathbf{G}}^H)^{-1} &= \hat{\mathbf{\Theta}}(\theta_{des}, \varphi_{des})\mathbf{G}_{opt}\hat{\mathbf{G}}^H(\hat{\mathbf{G}}\hat{\mathbf{G}}^H)^{-1}. \end{aligned} \quad (42)$$

From this point, we get (23).

## REFERENCES

- [1] S. Geng *et al.*, "Millimeter-wave propagation channel characterization for short-range wireless communications," *IEEE Trans. Veh. Technol.*, vol. 58, no. 1, pp. 3–13, 2008.
- [2] E. Basar *et al.*, "Wireless communications through reconfigurable intelligent surfaces," *IEEE Access*, vol. 7, pp. 116 753–116 773, 2019.
- [3] Ö. Özdoğan, E. Björnson, and E. G. Larsson, "Intelligent reflecting surfaces: Physics, propagation, and pathloss modeling," *IEEE Wireless Commun. Lett.*, 2019.
- [4] E. Björnson, Ö. Özdoğan, and E. G. Larsson, "Reconfigurable intelligent surfaces: Three myths and two critical questions," *arXiv preprint arXiv:2006.03377*, 2020.
- [5] Q. Wu and R. Zhang, "Intelligent reflecting surface enhanced wireless network via joint active and passive beamforming," *IEEE Trans. Wireless Commun.*, vol. 18, no. 11, pp. 5394–5409, 2019.
- [6] A. Taha, M. Alrabeiah, and A. Alkhateeb, "Enabling large intelligent surfaces with compressive sensing and deep learning," *arXiv preprint arXiv:1904.10136*, 2019.
- [7] Z.-Q. He and X. Yuan, "Cascaded channel estimation for large intelligent metasurface assisted massive MIMO," *IEEE Wireless Commun. Lett.*, 2019.
- [8] B. Zheng and R. Zhang, "Intelligent reflecting surface-enhanced OFDM: Channel estimation and reflection optimization," *IEEE Wireless Commun. Lett.*, 2019.
- [9] T. L. Jensen and E. De Carvalho, "An optimal channel estimation scheme for intelligent reflecting surfaces based on a minimum variance unbiased estimator," in *ICASSP 2020-2020 IEEE Int. Conf. Acoust., Speech and Signal Process. (ICASSP), Barcelona, Spain, Spain*. IEEE, 2020, pp. 5000–5004.
- [10] H. Alwazani *et al.*, "Intelligent reflecting surface-assisted multi-user MISO communication: Channel estimation and beamforming design," *IEEE Open J. Commun. Soc.*, vol. 1, pp. 661–680, 2020.
- [11] C. You, B. Zheng, and R. Zhang, "Intelligent reflecting surface with discrete phase shifts: Channel estimation and passive beamforming," in *ICC 2020-2020 IEEE Int. Conf. Commun. (ICC), Dublin, Ireland*. IEEE, 2020, pp. 1–6.
- [12] H. Alwazani *et al.*, "Intelligent reflecting surface-assisted multi-user MISO communication: Channel estimation and beamforming design," *IEEE Open J. Commun. Soc.*, vol. 1, pp. 661–680, 2020.
- [13] Z. Wang, L. Liu, and S. Cui, "Channel estimation for intelligent reflecting surface assisted multiuser communications: Framework, algorithms, and analysis," *IEEE Trans. Wireless Commun.*, 2020.
- [14] Z. Wan, Z. Gao, and M.-S. Alouini, "Broadband channel estimation for intelligent reflecting surface aided mmWave massive MIMO systems," *arXiv preprint arXiv:2002.01629*, 2020.
- [15] W. Tang *et al.*, "Wireless communications with reconfigurable intelligent surface: Path loss modeling and experimental measurement," *arXiv preprint arXiv:1911.05326*, 2019.
- [16] P. Wang *et al.*, "Compressed channel estimation and joint beamforming for intelligent reflecting surface-assisted millimeter wave systems," *arXiv preprint arXiv:1911.07202*, 2019.
- [17] T. Lin *et al.*, "Channel estimation for intelligent reflecting surface-assisted millimeter wave MIMO systems," *arXiv preprint arXiv:2005.04720*, 2020.
- [18] X. Ma *et al.*, "Joint channel estimation and data rate maximization for intelligent reflecting surface assisted terahertz MIMO communication systems," *IEEE Access*, 2020.
- [19] P. Wang, J. Fang, H. Duan, and H. Li, "Compressed channel estimation for intelligent reflecting surface-assisted millimeter wave systems," *IEEE Signal Process. Lett.*, 2020.
- [20] C. Jia *et al.*, "High-resolution channel estimation for intelligent reflecting surface-assisted mmWave communications," *arXiv preprint arXiv:2006.11730*, 2020.
- [21] C. Hu *et al.*, "Super-resolution channel estimation for mmwave massive MIMO with hybrid precoding," *IEEE Trans. Veh. Technol.*, vol. 67, no. 9, pp. 8954–8958, 2018.
- [22] M. Di Renzo *et al.*, "Analytical modeling of the path-loss for reconfigurable intelligent surfaces—anomalous mirror or scatterer?" *arXiv preprint arXiv:2001.10862*, 2020.
- [23] A. Goldsmith, *Wireless communications*. Cambridge university press, 2005.
- [24] L. Liang, W. Xu, and X. Dong, "Low-complexity hybrid precoding in massive multiuser MIMO systems," *IEEE Wireless Commun. Lett.*, vol. 3, no. 6, pp. 653–656, 2014.
- [25] R. W. Heath *et al.*, "An overview of signal processing techniques for millimeter wave MIMO systems," *IEEE J. Sel. Areas Commun.*, vol. 10, no. 3, pp. 436–453, 2016.
- [26] D. Zhu, J. Choi, and R. W. Heath, "Auxiliary beam pair enabled AoD and AoA estimation in closed-loop large-scale millimeter-wave MIMO systems," *IEEE Trans. Wireless Commun.*, vol. 16, no. 7, pp. 4770–4785, 2017.
- [27] J. Lee, G.-T. Gil, and Y. H. Lee, "Channel estimation via orthogonal matching pursuit for hybrid MIMO systems in millimeter wave communications," *IEEE Trans. Commun.*, vol. 64, no. 6, pp. 2370–2386, 2016.
- [28] X. Wu, N. C. Beaulieu, and D. Liu, "On favorable propagation in massive MIMO systems and different antenna configurations," *IEEE Access*, vol. 5, pp. 5578–5593, 2017.
- [29] W. Tan *et al.*, "Analysis of different planar antenna arrays for mmWave massive MIMO systems," in *2017 IEEE 85th Veh. Technol. Conf. (VTC Spring), Sydney, NSW, Australia*. IEEE, 2017, pp. 1–5.
- [30] Z. Xiao *et al.*, "Hierarchical codebook design for beamforming training in millimeter-wave communication," *IEEE Trans. Wireless Commun.*, vol. 15, no. 5, pp. 3380–3392, 2016.
- [31] W. Wu *et al.*, "Two-stage 3D codebook design and beam training for millimeter-wave massive MIMO systems," in *2017 IEEE 85th Veh. Technol. Conf. (VTC Spring), Sydney, NSW, Australia*. IEEE, 2017, pp. 1–7.
- [32] S. Jayaprakasam *et al.*, "Robust beam-tracking for mmWave mobile communications," *IEEE Commun. Lett.*, vol. 21, no. 12, pp. 2654–2657, 2017.
- [33] J. Fang *et al.*, "Super-resolution compressed sensing for line spectral estimation: An iterative reweighted approach," *IEEE Trans. Signal Process.*, vol. 64, no. 18, pp. 4649–4662, 2016.
- [34] C. Zhang, D. Guo, and P. Fan, "Tracking angles of departure and arrival in a mobile millimeter wave channel," in *Proc. IEEE Int. Conf. Commun. (ICC), Kuala Lumpur, Malaysia*. IEEE, 2016, pp. 1–6.
- [35] V. Va, H. Vikalo, and R. W. Heath, "Beam tracking for mobile millimeter wave communication systems," in *Proc. IEEE Global Conf. Signal and Inf. Process. (GlobalSIP), Washington, DC, USA*. IEEE, 2016, pp. 743–747.
- [36] Y. Yapıcı and I. Güvenç, "Low-complexity adaptive beam and channel tracking for mobile mmWave communications," in *Proc. 52nd Asilomar Conference on Signals, Systems, and Computers, Pacific Grove, CA, USA*. IEEE, 2018, pp. 572–576.
- [37] A. Rozé *et al.*, "Comparison between a hybrid digital and analog beamforming system and a fully digital massive MIMO system with adaptive beamsteering receivers in millimeter-wave transmissions," in *2016 International Symposium on Wireless Communication Systems (ISWCS), Poznan, Poland*. IEEE, 2016, pp. 86–91.
- [38] V. Arun and H. Balakrishnan, "RFocus: Beamforming using thousands of passive antennas," in *17th {USENIX} Symposium on Networked Systems Design and Implementation ({NSDI} 20)*. Santa Clara, CA: USENIX Association, Feb. 2020, pp. 1047–1061. [Online]. Available: <https://www.usenix.org/conference/nsdi20/presentation/arun>